Glaucoma Diagnostic Ability of Layer-by-Layer Segmented Ganglion Cell Complex by Spectral-Domain Optical Coherence Tomography

Hae Jin Kim,[1] Sang-Yoon Lee,[2] Ki Ho Park,[1] Dong Myung Kim,[1] and Jin Wook Jeoung[1]

[1]Department of Ophthalmology, Seoul National University Hospital, Seoul National University College of Medicine, Seoul, Korea
[2]Department of Ophthalmology, Jeju National University Hospital, Jeju National University College of Medicine, Jeju, Korea

Correspondence: Jin Wook Jeoung, Department of Ophthalmology, Seoul National University Hospital, Seoul National University College of Medicine, 101 Daehak-ro, Jongno-gu, Seoul 110-744, Korea; neuroprotect@gmail.com.

Submitted: January 25, 2016
Accepted: August 7, 2016

Citation: Kim HJ, Lee S-Y, Park KH, Kim DM, Jeoung JW. Glaucoma diagnostic ability of layer-by-layer segmented ganglion cell complex by spectral-domain optical coherence tomography. *Invest Ophthalmol Vis Sci*. 2016;57:4799–4805. DOI: 10.1167/iovs.16-19214

Purpose. To evaluate the diagnostic ability of layer-by-layer segmented macular ganglion cell complex (GCC) using spectral-domain optical coherence tomography (OCT) for detection of glaucoma and to analyze the topographic patterns of the segmented thicknesses in open-angle glaucoma.

Methods. Seventy-seven open-angle glaucoma patients and 59 healthy subjects were enrolled in this cross-sectional study. Spectral-domain OCT with automated segmentation was used to measure the separate thicknesses of macular retinal nerve fiber layer (mRNFL), ganglion cell layer (GCL), and inner plexiform layer (IPL). We compared the specific diagnostic abilities of the GCC (RNFL+GCL+IPL), ganglion cell–inner plexiform layer (GCIPL: GCL+IPL), and circumpapillary RNFL (cpRNFL) to discriminate between normal eyes and glaucoma.

Results. The mRNFL, GCL, IPL, and cpRNFL thicknesses in glaucoma patients were all significantly thinner compared with healthy subjects and showed different topographic patterns. The GCC, mRNFL, and GCL thicknesses were best able to discriminate between the glaucoma and normal groups. The areas under the curve of receiver operating characteristics (AUROCs) of the mRNFL and GCL did not show significant difference from that of the cpRNFL. The AUROC of the GCL did not show significant difference from that of GCIPL after Bonferroni correction. The global IPL thickness had the smallest AUROC and showed lower diagnostic performance than the GCL, GCIPL, and GCC.

Conclusions. The diagnostic ability of segmented mRNFL and GCL to discriminate between normal and glaucoma eyes is high and comparable to that of cpRNFL thickness. The measurement and monitoring of GCL could be a practical and effective approach to glaucoma diagnostics.

Keywords: glaucoma, macular ganglion cell complex, spectral-domain optical coherence tomography, segmented ganglion cell complex

Glaucoma preferentially affects the ganglion cell complex (GCC), which is the sum of the three innermost layers: the retinal nerve fiber layer (RNFL), which is composed of ganglion cell axons, neuroglia, and astrocytes; the ganglion cell layer (GCL), which is composed of cell bodies; and the inner plexiform layer (IPL), which contains the retinal ganglion cell dendrites.[1] Conventionally, the loss of retinal ganglion cells in glaucoma has been evaluated based on circumpapillary RNFL (cpRNFL) thinning and neuroretinal rim narrowing of the optic nerve head.[1–5] These assessments, however, cannot exactly reflect the extent to which the GCC is affected.

Recent advances in segmentation algorithms have enabled better quantitative GCC assessment for effective diagnosis and evaluation of glaucoma progression.[1,6,7] Previous studies have used the Cirrus spectral-domain optical coherence tomography (OCT) ganglion cell analysis (GCA) algorithm, swept-source OCT segmentation software (version 9.12),[8] or RTVue-100 OCT software (version 6.3),[9] all of which measure the thickness of the macular ganglion cell–inner plexiform layer (GCIPL) or GCC. Notwithstanding the importance and effectiveness of GCC analysis for glaucoma, well documented in many studies, there are few reports on layer-by-layer segmented GCC analysis. Some studies attempted manual segmentation for separate measurement of GCC thickness,[10] or automated layer-by-layer segmentation technique was used for the analysis in multiple sclerosis patients.[11]

Spectralis OCT (Heidelberg Engineering, Inc., Heidelberg, Germany; software version 6.0) has introduced an automated segmentation algorithm that allows for successful and reproducible segmentation of the 10 retinal layers. By means of this technology, it is possible to separately evaluate the RNFL, GCL, and IPL thicknesses within the central posterior pole. Recently, Ctori and Huntjens,[12] using Spectralis OCT segmentation software, demonstrated excellent repeatability and reproducibility for each of eight individual retinal layer thickness measurements within the fovea. Dysli et al.[13] revealed that this automated retinal segmentation algorithm performed well for the inner layers in mice. Because glaucoma primarily affects the retinal ganglion cells, the separate measurement of GCC may enable early detection of glaucoma and direct evaluation of glaucomatous damage.

The present study was designed to evaluate the diagnostic ability of layer-by-layer segmented macular GCC for detection of glaucoma and to analyze the topographic pattern of segmented thicknesses in glaucoma patients compared with healthy subjects.

Methods

Subjects

A total of 136 subjects (77 eyes of 77 open-angle glaucoma patients and 59 eyes of 59 healthy subjects) were enrolled from the Glaucoma Clinic of Seoul National University Hospital. Informed consent was obtained from all of the subjects. This study adhered to the tenets of the Declaration of Helsinki and was approved by the Institutional Review Board of Seoul National University Hospital, Korea.

All of the subjects underwent a comprehensive ophthalmic examination, including visual acuity and refraction, intraocular pressure (IOP) measurement with Goldmann tonometry, dilated fundus examination, and standard automated perimetry (SAP) (Humphrey field analyzer II; Carl Zeiss Meditec, Dublin, CA, USA) testing. All were familiar with SAP from earlier experience of at least two visual field (VF) tests. Manifest refractions were recorded with an automatic refractometer (RK-F1; Topcon Corporation, Tokyo, Japan). All the optic disc and red-free RNFL photographs were obtained with a digital fundus camera (CF-60UVI; Canon, Tokyo, Japan).

All of the participants in this study met the following inclusion criteria: best-corrected visual acuity of 20/40 or better, spherical-equivalent refractive error within ±6.00 diopters and astigmatism within ±3.00 diopters, open anterior chamber angle on slit-lamp and gonioscopic examinations, and good-quality fundus images. To be eligible, if subjects had a history of cataract surgery, the subjects needed to have a minimum interval of 6 months after surgery. In cases in which both eyes were eligible, one eye was randomly selected.

The following individuals were excluded: those with a history of intraocular surgery including trabeculectomy or Ahmed valve implantation, except uncomplicated cataract surgery; those with any other ocular disease (i.e., age-related macular degeneration, epiretinal membrane, macular edema); and those with other optic nerve disease excepting glaucoma (e.g., ischemic optic neuropathy, multiple sclerosis).

A normal subject was defined as having an IOP less than 22 mm Hg with no history of increased IOP, a normal VF result on at least two SAP tests, and no visible RNFL defect on red-free fundus photography. Diagnosis of glaucoma was determined based on a finding of glaucomatous VF defect confirmed by three consecutive reliable SAP measurements and the presence of glaucomatous optic disc cupping irrespective of IOP. Glaucomatous optic disc cupping was defined as neuroretinal rim thinning, notching, excavation, or RNFL defect with a corresponding VF deficit. Photographs of the optic disc and red-free RNFL were independently evaluated by two observers (HJK and JWJ) in random order and in a masked fashion, without knowledge of clinical information. Any discrepancy between the observers was resolved by consensus. The severity of glaucomatous damage was classified into early and moderate-to-severe according to the Hodapp-Parrish-Anderson criterion.[14]

Spectralis Optical Coherence Tomography

Spectralis OCT can calculate the segmented retinal thicknesses of 64 sectors in the posterior pole by use of software version 6.0. In the current study, Spectralis OCT was performed by a single experienced examiner (HJK) after pharmacologic dilation of the pupil.

With the anatomic positional system (APS), two fixed anatomic landmarks, namely, the fovea and the Bruch's membrane opening (BMO) center, are located. Then, the APS automatically aligns each patient's OCT scan relative to the fovea to BMO center axis. For analysis of the macular GCC, we obtained confocal scanning laser ophthalmoscopy (cSLO) images on each of which a 8×8 posterior pole grid was superimposed (Fig. 1). Confocal SLO generates a topographic map by analyzing the light peak reflectance of the retinal surface as captured with a confocal photodetector. With APS scans, the center of the grid superimposed on the cSLO image is positioned on the fovea symmetrically to the fovea-to-disc axis. This grid shows the retinal thickness over the entire $30° \times 25°$ OCT posterior pole volume scan. In each grid cell, the mean retinal layer thickness is displayed in micrometers. The width and height of a cell is 860 μm, corresponding to a 3° scan angle. The quality of the scans is indicated in decibels in the right bottom of the images: More than 25 decibels is required for an image to be considered of sufficiently good quality.

Quality assessments of the OCT scans were performed by using the criteria of Ishikawa et al.[15] In detail, we excluded eyes with segmentation failures, which were defined as obvious disruption of the detected border, and/or border wandering (detected border jumping to and from different anatomic structures), within >5% consecutively (i.e., an uninterrupted error) or 20% cumulatively (i.e., adding up all errors amounted to 20% of the image width) of the entire image.

The designation of the 8×8 posterior pole grid section was as shown in Figure 1. The global average thickness of each layer was calculated according to the average thickness of 64 cells. The superonasal thickness was calculated as an averaged value for 16 cells (designated numbers: 11–14, 21–24, 31–34, 41–44). In the same way, the superotemporal thickness was calculated according to the average thickness of 16 cells (designated numbers: 15–18, 25–28, 35–38, 45–48), as were the inferonasal (51–54, 61–64, 71–74, 81–84) and inferotemporal (55–58, 65–68, 75–78, 85–88) thicknesses.

An earlier study having demonstrated excellent interobserver and intervisit reproducibilities for this posterior pole analysis,[16] just one scan was used to measure the retinal thicknesses of the 64 cells, and no manual correction was applied to the outcome.

Data Analysis

Statistical analyses were performed using SPSS software (version 20.0; SPSS, Inc., Chicago, IL, USA). The sex and laterality differences between the normal and glaucoma groups were compared by Pearson χ^2 test. Age, IOP, spherical equivalent, and central corneal thickness were compared by *t*-test. The cpRNFL, macular retinal nerve fiber layer (mRNFL), GCL, IPL, GCIPL (sum of GCL and IPL), and GCC (sum of mRNFL, GCL and IPL) thicknesses between two groups were compared by *t*-test. For multiple comparisons, the Bonferroni correction was used to adjust for type I error. The mRNFL, GCL, IPL, GCIPL, and GCC parameters were analyzed on two different levels: global average and quadrant (superonasal, superotemporal, inferonasal, inferotemporal). The areas under the curve of receiver operating characteristics (AUROCs) were used to investigate the ability of each parameter to discriminate glaucomatous from healthy eyes. An AUROC of 1.0 represents perfect discrimination, whereas an AUROC of 0.5 represents chance discrimination. The AUROCs of different variables were compared using MedCalc software version 11.0 (MedCalc Statistical Software, Marakierke, Belgium). To test for the statistical significance of performance difference between any two parameters, DeLong's test was used to compare the

Investigative Ophthalmology & Visual Science

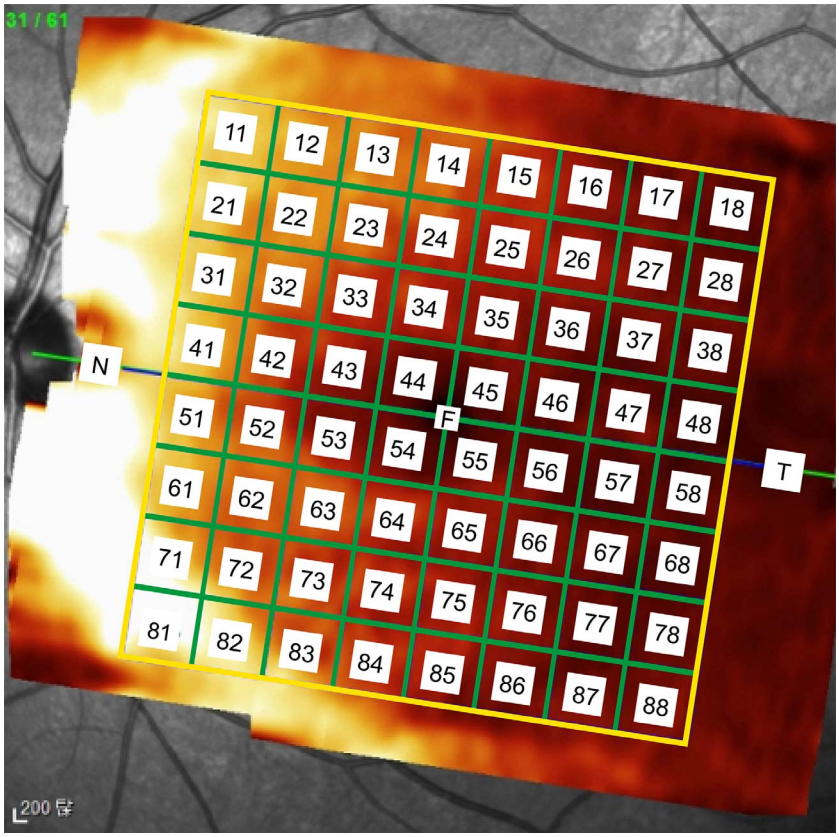

Figure 1. Designation of 8 × 8 posterior pole grid section.

AUROCs.[17] *P* values less than 0.05 were considered to be statistically significant.

Results

This study initially included 147 eyes of 147 subjects (63 healthy subjects and 84 glaucoma patients). We excluded five subjects because of epiretinal membrane ($n = 3$) and macular degeneration ($n = 2$). Of the remaining 142 eyes, 6 eyes (4.22%) with OCT segmentation failure were excluded from further analysis. Therefore, the final study sample included 136 eyes of 136 subjects (59 healthy subjects and 77 glaucoma patients).

Subject Baseline Characteristics

The baseline demographics are summarized in Table 1. All subjects were Korean. The mean subject age was 58.7 ± 9.9 years (range, 29–77 years). There was no significant difference in the mean age between the normal control subjects (57.0 ± 9.7 years) and glaucoma patients (60.0 ± 9.8 years). Neither sex, laterality, best-corrected visual acuity, IOP, spherical equivalent, nor central corneal thickness showed any differences between the two groups (all $P > 0.05$). According to the Hodapp-Parrish-Anderson classification, the glaucoma patients were classified as having early ($n = 50$) and moderate-to-severe ($n = 27$) glaucoma. There were significant differences in mean deviation (MD) and pattern standard deviation (PSD) values between the two groups (all $P < 0.001$) (Table 1).

Comparisons of Circumpapillary Retinal Nerve Fiber Layer and Segmented Macular Ganglion Cell Complex Thicknesses

As expected, cpRNFL thickness was significantly thinner in the glaucoma group than in the healthy subjects. The mRNFL,

Table 1. Demographics and Ocular Characteristics of Subjects

	Normal Group, $n = 59$, Mean ± Standard Deviation	Glaucoma Group, $n = 77$, Mean ± Standard Deviation	*P* Value
Sex, male:female	26:33	39:38	0.491*
Laterality, right:left	33:26	37:40	0.391*
Age, y	57.0 ± 9.7	60.0 ± 9.8	0.081†
BCVA, logMAR	0.04 ± 0.12	0.07 ± 0.12	0.140†
Mean IOP, mm Hg	14.00 ± 2.46	13.12 ± 3.14	0.082†
Spherical equivalent, diopters	−1.13 ± 2.31	−1.28 ± 2.17	0.552†
Mean CCT, μm	541.78 ± 35.61	531.76 ± 41.50	0.309†
MD	−0.23 ± 1.32	−5.47 ± 6.79	<0.001†
PSD	1.74 ± 0.47	6.11 ± 4.79	<0.001†

* Pearson χ^2 test.
† *t*-test.

Table 2. Thicknesses of Circumpapillary Retinal Nerve Fiber Layer, Macular Retinal Nerve Fiber Layer, Ganglion Cell Layer, Inner Plexiform Layer, Ganglion Cell–Inner Plexiform Layer, and Ganglion Cell Complex (μm) in Normal and Glaucoma Groups

Analytical Layer	Normal Group, $n = 59$, Mean ± Standard Deviation	Glaucoma Group, $n = 77$, Mean ± Standard Deviation	Unadjusted P Value*	Adjusted P Value After Bonferroni Correction
cpRNFL	99.42 ± 18.39	76.59 ± 19.58	<0.0001	<0.0001†
mRNFL				
Global	40.05 ± 4.79	30.04 ± 5.86	<0.0001	<0.0001†
SN	51.35 ± 8.68	41.42 ± 10.31	<0.0001	<0.0001†
ST	22.12 ± 2.70	20.05 ± 2.82	0.000031	0.0008†
IN	59.54 ± 6.98	38.11 ± 13.32	<0.0001	<0.0001†
IT	27.20 ± 3.17	20.56 ± 4.87	<0.0001	<0.0001†
GCL				
Global	32.02 ± 2.15	26.89 ± 3.36	<0.0001	<0.0001†
SN	33.34 ± 2.32	30.41 ± 3.80	<0.0001	<0.0001†
ST	30.95 ± 2.79	25.02 ± 4.67	<0.0001	<0.0001†
IN	31.71 ± 2.59	25.73 ± 4.59	<0.0001	<0.0001†
IT	32.26 ± 2.22	28.16 ± 3.90	<0.0001	<0.0001†
IPL				
Global	26.89 ± 1.59	24.58 ± 1.81	<0.0001	<0.0001†
SN	27.00 ± 1.82	25.53 ± 2.58	0.000293	0.0076†
ST	28.16 ± 1.95	25.60 ± 2.31	<0.0001	<0.0001†
IN	25.93 ± 1.85	24.09 ± 2.24	0.000001	<0.0001†
IT	26.48 ± 1.85	23.12 ± 2.19	<0.0001	<0.0001†
GCIPL				
Global	58.92 ± 3.68	51.42 ± 4.96	<0.0001	<0.0001†
SN	60.35 ± 4.04	55.94 ± 6.04	0.000004	0.0001†
ST	59.12 ± 2.27	51.34 ± 6.66	<0.0001	<0.0001†
IN	58.21 ± 1.96	52.04 ± 6.08	<0.0001	<0.0001†
IT	58.02 ± 2.02	46.34 ± 6.86	<0.0001	<0.0001†
GCC				
Global	98.98 ± 7.01	81.42 ± 10.08	<0.0001	<0.0001†
SN	111.70 ± 10.55	97.36 ± 15.23	<0.0001	<0.0001†
ST	81.25 ± 6.41	71.39 ± 8.90	<0.0001	<0.0001†
IN	117.75 ± 8.45	90.06 ± 17.30	<0.0001	<0.0001†
IT	85.22 ± 5.57	66.89 ± 10.95	<0.0001	<0.0001†

SN, superonasal; ST, superotemporal; IN, inferonasal; IT, inferotemporal.
* P using t-test.
† Statistically significant after Bonferroni correction.

GCL, and IPL thicknesses globally and in four quadrants were all significantly thinner in the glaucoma patients than in the healthy subjects after Bonferroni correction (all $P < 0.05$) (Table 2).

Diagnostic Ability of Segmented Macular Ganglion Cell Complex

The diagnostic abilities of the various OCT parameters for detection of glaucoma are presented in Table 3. Among the global average thicknesses, the global GCC (AUROC = 0.925), global mRNFL (AUROC = 0.915), and global GCL (AUROC = 0.914) were best able to discriminate between the glaucoma and normal groups. As for the quadrant parameters, the five best AUROCs for glaucoma detection were inferotemporal GCL (0.938), inferotemporal GCIPL (0.929), inferonasal GCC (0.926), inferotemporal GCC (0.922), and inferonasal mRNFL (0.914). Among the AUCs of these five best parameters, there were no significant differences (all $P > 0.05$).

The AUROCs of the global mRNFL and global GCL (0.915 and 0.914) tended to be larger than those of the cpRNFL (0.878), though the differences did not rise to statistical significance. The AUROC of the GCL was significantly larger than that of the GCIPL (0.914 vs. 0.895, $P = 0.016$), but was not significant after Bonferroni correction (corrected P value = 0.24) (Table 4; Fig. 2). The global IPL thickness had the smallest AUROCs and showed inferior diagnostic performance compared to those of the GCL, GCIPL, and GCC (all $P < 0.05$) (Table 4; Fig. 2).

Topographic Pattern of Reduced Macular Thickness in Separate Layers

The reduced thickness area of the mRNFL, GCL and IPL showed different topographic patterns (Fig. 3). The GCL thickness was reduced in nearly all of the 64 cells. The IPL thickness, in contrast, was reduced mainly in central posterior pole, while that of the RNFL was reduced mainly in the superior, inferior, and nasal posterior poles.

Discussion

The main objective of this study was to evaluate, using spectral-domain OCT, the glaucoma diagnostic ability of layer-by-layer segmented macular GCC and to analyze the topographic patterns of segmented thicknesses in open-angle glaucoma patients compared with healthy subjects. We confirmed that the diagnostic ability of segmented mRNFL and GCL to

Investigative Ophthalmology & Visual Science

Table 3. Area Under the Receiver Operating Characteristics Curve and Diagnostic Sensitivity of Circumpapillary Retinal Nerve Fiber Layer, Macular Retinal Nerve Fiber Layer, Ganglion Cell Layer, Inner Plexiform Layer, Ganglion Cell–Inner Plexiform Layer, Ganglion Cell Complex

		Sensitivity	
Analytical Layer	**AUROC (Standard Error)**	**Specificity Fixed at 90%**	**Specificity Fixed at 95%**
cpRNFL	0.878 (0.029)	65.97	58.18
mRNFL			
Global	0.915 (0.025)	79.22	68.83
SN	0.765 (0.040)	41.56	37.60
ST	0.727 (0.044)	42.73	21.88
IN	0.914 (0.027)	84.42	76.62
IT	0.880 (0.029)	75.32	70.13
GCL			
Global	0.914 (0.023)	75.32	68.83
SN	0.744 (0.041)	44.16	35.06
ST	0.839 (0.033)	64.94	58.44
IN	0.836 (0.033)	58.44	50.65
IT	0.938 (0.019)	84.42	76.62
IPL			
Global	0.836 (0.034)	57.14	50.58
SN	0.702 (0.044)	36.36	27.21
ST	0.798 (0.037)	55.58	44.09
IN	0.739 (0.042)	41.56	25.97
IT	0.887 (0.028)	72.73	41.49
GCIPL			
Global	0.895 (0.026)	67.53	64.94
SN	0.732 (0.042)	42.86	33.77
ST	0.831 (0.034)	64.81	54.55
IN	0.814 (0.036)	57.14	46.75
IT	0.929 (0.021)	84.42	67.53
GCC			
Global	0.925 (0.021)	83.12	70.13
SN	0.775 (0.039)	53.25	41.56
ST	0.812 (0.036)	62.34	57.14
IN	0.926 (0.023)	84.42	76.62
IT	0.922 (0.023)	84.42	80.52

SN, superonasal; ST, superotemporal; IN, inferonasal; IT, inferotemporal.

differentiate between normal eyes and glaucoma is high and comparable to that of cpRNFL thickness. Moreover, no significant difference was found between the diagnostic ability of GCL and that of GCIPL.

Recent studies have shown that measurement of retinal ganglion cell loss in the macular area can be a direct and powerful method for glaucoma diagnosis.[1,6,7] As expected, our results showed significantly decreased RNFL, GCL, and IPL thicknesses in open-angle glaucoma patients relative to healthy subjects (all $P \leq 0.05$). Additionally, and consistently with relevant previous reports, our data showed a high diagnostic performance for GCC. Among the global average thicknesses, the global GCC (AUROC = 0.925) and global mRNFL (AUROC = 0.915) were best able to discriminate between glaucoma and normal subjects. The global GCL thickness also showed a large AUROC (0.914), which value was not significantly different from those for the global GCC and mRNFL. Because glaucoma primarily affects retinal ganglion cells and their axons, separate GCL and mRNFL measurement can be an effective direct method for glaucoma diagnosis in clinical settings.

The present study's comparison of the mRNFL (0.915), GCL (0.914), and cpRNFL (0.878) AUROCs did not show any significant difference. This finding implies that the ability of segmented mRNFL and GCL to discriminate normal and glaucomatous eyes is high and comparable to that of cpRNFL thickness. In fact, our results correspond well with those of the earlier Cirrus OCT study that reported similar glaucoma diagnostic abilities for GCIPL parameters and cpRNFL thickness.[18,19] In contrast to Cirrus OCT, however, which measures GCIPL thickness within a 14.13-mm^2 elliptical annulus area centered on the fovea, Spectralis OCT, employed in the present study, can measure a broader area. Indeed, the area of the 8×8 posterior pole grid in Spectralis OCT is approximately 47.33 mm^2, based on the width and height of one cell, 860 μm. Further studies on the diagnostic performance of GCC analysis according to scan area will be needed.

Interestingly, in the present study, the global IPL thickness showed the smallest AUROC (0.836) and inferior diagnostic ability to GCL, GCIPL, and GCC (all $P < 0.05$). In addition, the diagnostic ability of GCL did not show significant difference from that of GCIPL after Bonferroni correction. This result is thought to have been due to the inferior diagnostic ability of IPL thickness. In IPL, retinal ganglion cell dendrites synapse on the axon terminals of bipolar cells.[20] Retinal ganglion cell dendrites, unlike axons, which are unable to regenerate after birth, have demonstrated a postinjury capacity to increase their dendritic receptive field and develop new dendritic branches.[21–23] Park et al.,[24] utilizing an experimental glaucoma model, recently demonstrated that in the IPL, even though retinal ganglion cells undergo apoptosis and the synapses decrease in total number, the synaptic formations between retinal ganglion cells and bipolar cells increase. This finding might account for the present finding that IPL thickness had the smallest AUROCs among the segmented layer parameters in discriminating glaucoma from normal eyes.

In this study, the glaucomatous mRNFL, GCL and IPL changes showed different topographic patterns. As is consis-

Table 4. Comparison of Area Under the Receiver Operating Characteristics Curves Among Global Average Thicknesses of Different Parameters

		Comparison of AUROC				
		Unadjusted *P* Value / Adjusted *P* Value After Bonferroni Correction				
Analytical Layer	**AUROC**	**vs. cpRNFL**	**vs. mRNFL**	**vs. GCL**	**vs. IPL**	**vs. GCIPL**
GCC	0.925	0.080 / NS	0.470 / NS	0.491 / NS	**0.002 / 0.03**	0.110 / NS
GCIPL	0.895	0.601 / NS	0.524 / NS	**0.016** / 0.24	**0.0001 / 0.0015**	
IPL	0.836	0.273 / NS	**0.048** / 0.72	**0.0003 / 0.0045**		
GCL	0.914	0.231 / NS	0.988 / NS			
mRNFL	0.915	0.216 / NS				
cpRNFL	0.878					

$P < 0.05$ shown in boldface. NS, not significant.

Investigative Ophthalmology & Visual Science

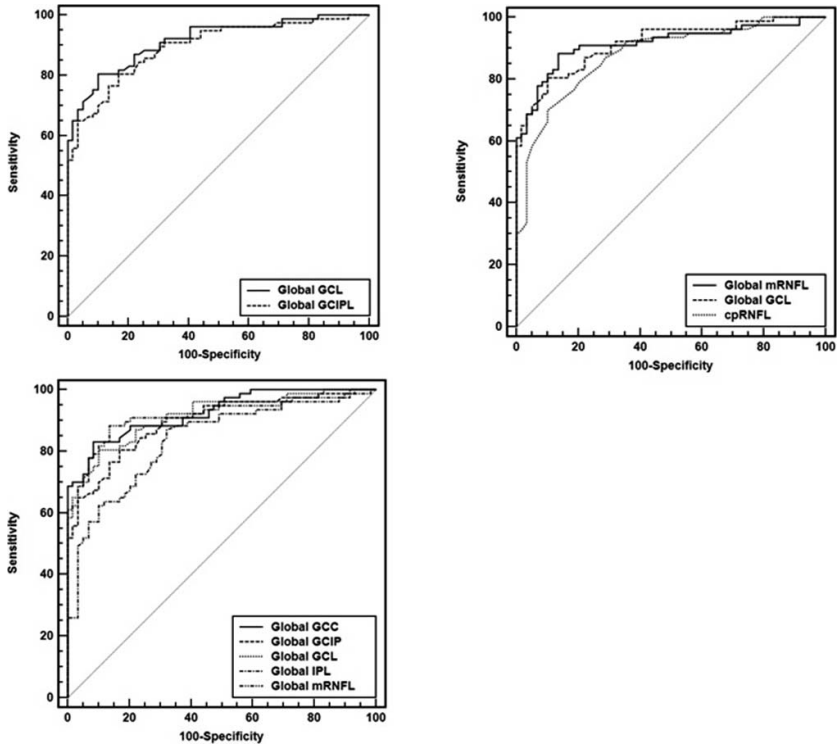

Figure 2. Area under the curve of receiver operating characteristics (AUROCs) of global average circumpapillary retinal nerve fiber layer (cpRNFL), macular retinal nerve fiber layer (mRNFL), ganglion cell layer (GCL), inner plexiform layer (IPL), ganglion cell–inner plexiform layer (GCIPL), and ganglion cell complex (GCC). (**A**) The AUROC of the GCL was significantly larger than that of GCIPL (0.914 vs. 0.895, $P = 0.016$), but was not significant after Bonferroni correction (corrected P value = 0.24). (**B**) The AUROCs of the mRNFL and GCL (0.915 and 0.914) tended to be larger than the circumpapillary RNFL (0.878), but the difference did not reach statistical significance. (**C**) The global IPL thickness showed the smallest AUROCs as well as inferior diagnostic ability relative to macular GCL, GCIPL, and GCC (all $P < 0.05$).

tent with previous experimental glaucoma models showing substantial GCL loss in the peri- and parafoveal regions,[25,26] the GCL thicknesses were reduced in nearly all 64 cells. The IPL thicknesses, by contrast, were reduced mainly in the central posterior pole, and those of the RNFL were reduced mainly in the superior, inferior, and nasal quadrants. These topographic findings also have significant implications. The area of reduced mRNFL thickness did not match perfectly with that of reduced GCL thickness. This might have been due to the fact that the RNFL contains fibers from many other different locations. The local RNFL, in other words, is not a measure of local retinal ganglion cell loss. Although the diagnostic ability of the mRNFL did not show significant difference from the GCL in this study, it seems that GCL analysis can have a major role in the detection of early glaucoma.

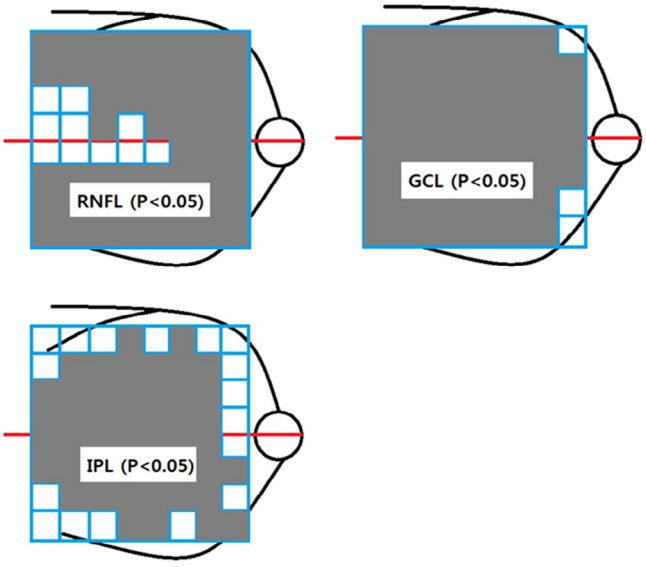

Figure 3. Topographic patterns of reduced retinal nerve fiber layer (RNFL), ganglion cell layer (GCL), and inner plexiform layer (IPL) thicknesses for 64 cells in the posterior pole. Comparisons of the thicknesses between the glaucoma and normal groups were performed by *t*-test. The areas of significant differences ($P < 0.05$) are shown in *gray*.

There are several limitations to this study. First, all study subjects were Korean and thus lacked ethnic variety. Asians have been reported to have thicker RNFL values in some locations relative to Caucasians.[27,28] Also, it is possible to have greater diagnostic abilities of GCIPL parameters in a Korean population because of a higher prevalence of normal-tension glaucoma in Koreans[29] with glaucomatous damage closer to fixation.[30] In fact, Kim et al.[31] reported that if the RNFL defects are located closer to the fovea, there are more chances for a macular GCIPL scan to detect them. Second, the relatively small number of subjects made it difficult to perform subgroup analysis according to the locations of VF damage[32] or the stages of glaucoma. In a large-sample study, more advanced analysis, such as correlation analysis between structural changes and functional readouts, will be necessary to improve our understandings of segmented GCC. Another weakness of our study is that we could not compare the diagnostic ability of the segmented algorithm of the Spectralis OCT with other manufacturers' OCT.

In conclusion, the ability of segmented mRNFL and GCL to discriminate between normal and glaucoma eyes is high and comparable to that of cpRNFL thickness. Also, there was no

significant difference between the diagnostic performance of the GCL and that of the GCIPL. Given the basic nature of glaucoma, specifically its manifestation of retinal ganglion cell loss, measurement and monitoring of the GCL could be a practical and effective approach to glaucoma diagnostics.

Acknowledgments

Disclosure: **H.J. Kim**, None; **S.-Y. Lee**, None; **K.H. Park**, None; **D.M. Kim**, None; **J.W. Jeoung**, None

References

1. Mwanza JC, Oakley JD, Budenz DL, Chang RT, Knight OJ, Feuer WJ. Macular ganglion cell-inner plexiform layer: automated detection and thickness reproducibility with spectral domain-optical coherence tomography in glaucoma. *Invest Ophthalmol Vis Sci*. 2011;52:8323–8329.
2. Sommer A, Katz J, Quigley HA, et al. Clinically detectable nerve fiber atrophy precedes the onset of glaucomatous field loss. *Arch Ophthalmol*. 1991;109:77–83.
3. Quigley HA, Addicks EM, Green WR. Optic nerve damage in human glaucoma. III. Quantitative correlation of nerve fiber loss and visual field defect in glaucoma, ischemic neuropathy, papilledema, and toxic neuropathy. *Arch Ophthalmol*. 1982; 100:135–146.
4. Quigley HA, Dunkelberger GR, Green WR. Retinal ganglion cell atrophy correlated with automated perimetry in human eyes with glaucoma. *Am J Ophthalmol*. 1989;107:453–464.
5. Airaksinen PJ, Tuulonen A, Alanko HI. Rate and pattern of neuroretinal rim area decrease in ocular hypertension and glaucoma. *Arch Ophthalmol*. 1992;110:206–210.
6. Mwanza JC, Durbin MK, Budenz DL, et al. Glaucoma diagnostic accuracy of ganglion cell-inner plexiform layer thickness: comparison with nerve fiber layer and optic nerve head. *Ophthalmology*. 2012;119:1151–1158.
7. Jeoung JW, Choi YJ, Park KH, Kim DM. Macular ganglion cell imaging study: glaucoma diagnostic accuracy of spectral-domain optical coherence tomography. *Invest Ophthalmol Vis Sci*. 2013;54:4422–4429.
8. Yang Z, Tatham AJ, Weinreb RN, Medeiros FA, Liu T, Zangwill LM. Diagnostic ability of macular ganglion cell inner plexiform layer measurements in glaucoma using swept source and spectral domain optical coherence tomography. *PLoS One*. 2015;10:e0125957.
9. Hollo G, Naghizadeh F. Influence of a new software version of the RTVue-100 optical coherence tomograph on ganglion cell complex segmentation in various forms of age-related macular degeneration. *J Glaucoma*. 2015;24:245–250.
10. Wang M, Hood DC, Cho JS, et al. Measurement of local retinal ganglion cell layer thickness in patients with glaucoma using frequency-domain optical coherence tomography. *Arch Ophthalmol*. 2009;127:875–881.
11. Garcia-Martin E, Polo V, Larrosa JM, et al. Retinal layer segmentation in patients with multiple sclerosis using spectral domain optical coherence tomography. *Ophthalmology*. 2014; 121:573–579.
12. Ctori I, Huntjens B. Repeatability of foveal measurements using Spectralis optical coherence tomography segmentation software. *PLoS One*. 2015;10:e0129005.
13. Dysli C, Enzmann V, Sznitman R, Zinkernagel MS. Quantitative analysis of mouse retinal layers using automated segmentation of spectral domain optical coherence tomography images. *Trans Vis Sci Tech*. 2015;4(4):9.
14. Hodapp E, Parrish RK II, Anderson DR. Clinical Decisions in Glaucoma. St. Louis, MO: Mosby; 1993:52–61.
15. Ishikawa H, Stein DM, Wollstein G, Beaton S, Fujimoto JG, Schuman JS. Macular segmentation with optical coherence tomography. *Invest Ophthalmol Vis Sci*. 2005;46:2012–2017.
16. Yamashita T, Tanaka M, Kii Y, Nakao K, Sakamoto T. Association between retinal thickness of 64 sectors in posterior pole determined by optical coherence tomography and axial length and body height. *Invest Ophthalmol Vis Sci*. 2013;54:7478–7482.
17. DeLong ER, DeLong DM, Clarke-Pearson DL. Comparing the areas under two or more correlated receiver operating characteristic curves: a nonparametric approach. *Biometrics*. 1988;44:837–845.
18. Begum VU, Addepalli UK, Yadav RK, et al. Ganglion cell-inner plexiform layer thickness of high definition optical coherence tomography in perimetric and preperimetric glaucoma. *Invest Ophthalmol Vis Sci*. 2014;55:4768–4775.
19. Kotowski J, Folio LS, Wollstein G, et al. Glaucoma discrimination of segmented cirrus spectral domain optical coherence tomography (SD-OCT) macular scans. *Br J Ophthalmol*. 2012; 96:1420–1425.
20. Kim HL, Jeon JH, Koo TH, et al. Axonal synapses utilize multiple synaptic ribbons in the mammalian retina. *PLoS One*. 2012;7:e52295.
21. Dancause N, Barbay S, Frost SB, et al. Extensive cortical rewiring after brain injury. *J Neurosci*. 2005;25:10167–10179.
22. Fisher SK, Lewis GP, Linberg KA, Verardo MR. Cellular remodeling in mammalian retina: results from studies of experimental retinal detachment. *Prog Retin Eye Res*. 2005; 24:395–431.
23. Sullivan RK, Woldemussie E, Pow DV. Dendritic and synaptic plasticity of neurons in the human age-related macular degeneration retina. *Invest Ophthalmol Vis Sci*. 2007;48: 2782–2791.
24. Park HY, Kim JH, Park CK. Alterations of the synapse of the inner retinal layers after chronic intraocular pressure elevation in glaucoma animal model. *Mol Brain*. 2014;7:53.
25. Desatnik H, Quigley HA, Glovinsky Y. Study of central retinal ganglion cell loss in experimental glaucoma in monkey eyes. *J Glaucoma*. 1996;5:46–53.
26. Frishman LJ, Shen FF, Du L, et al. The scotopic electroretinogram of macaque after retinal ganglion cell loss from experimental glaucoma. *Invest Ophthalmol Vis Sci*. 1996;37: 125–141.
27. Alasil T, Wang K, Keane PA, et al. Analysis of normal retinal nerve fiber layer thickness by age, sex, and race using spectral domain optical coherence tomography. *J Glaucoma*. 2013;22: 532–541.
28. Knight OJ, Girkin CA, Budenz DL, Durbin MK, Feuer WJ. Effect of race age, and axial length on optic nerve head parameters and retinal nerve fiber layer thickness measured by Cirrus HD-OCT. *Arch Ophthalmol*. 2012;130:312–318.
29. Kim CS, Seong GJ, Lee NH, Song KC. Prevalence of primary open-angle glaucoma in central South Korea the Namil study. *Ophthalmology*. 2011;118:1024–1030.
30. Kim DM, Seo JH, Kim SH, Hwang SS. Comparison of localized retinal nerve fiber layer defects between a low-teen intraocular pressure group and a high-teen intraocular pressure group in normal-tension glaucoma patients. *J Glaucoma*. 2007;16:293–296.
31. Kim MJ, Jeoung JW, Park KH, Choi YJ, Kim DM. Topographic profiles of retinal nerve fiber layer defects affect the diagnostic performance of macular scans in preperimetric glaucoma. *Invest Ophthalmol Vis Sci*. 2014;55:2079–2087.
32. Shin HY, Park HY, Jung KI, Choi JA, Park CK. Glaucoma diagnostic ability of ganglion cell-inner plexiform layer thickness differs according to the location of visual field loss. *Ophthalmology*. 2014;121:93–99.